	Experiment title: Local Structure of Natural X-Ray Amorphous Ferric Arsenates	**Experiment number**: EV-126
Beamline: BM20A	**Date of experiment**: From 12.02. to 17.02.2015	**Date of report**: 6 November 2015
Shifts: 18	**Local contact(s)**: Andreas Scheinost	*Received at ESRF:*

Names and affiliations of applicants (* indicates experimentalists):

Christian Mikutta[1,*]
Juraj Majzlan[2]

[1]Institute of Biogeochemistry and Pollutant Dynamics, Swiss Federal Institute of Technology Zurich, Switzerland
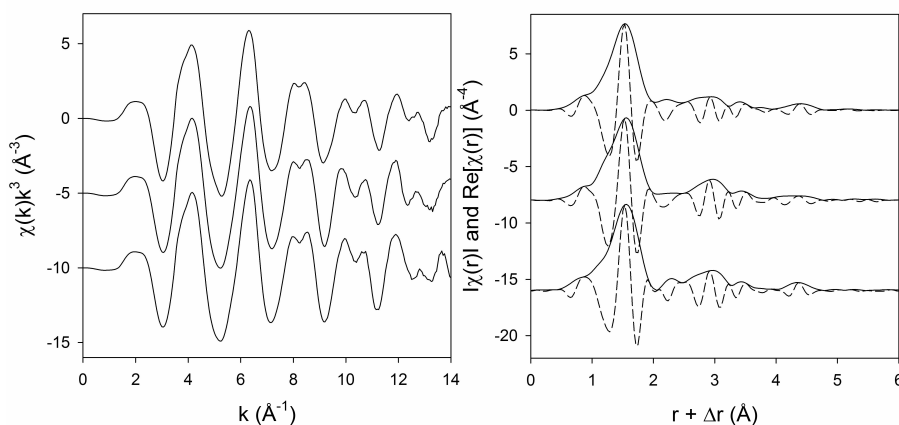[2]Institute of Geosciences, Friedrich-Schiller University of Jena, Germany

1. Background

Elevated concentrations of the ubiquitous and pervasive environmental toxin arsenic (As) in natural waters, soils, and sediments represent a major problem for millions of people worldwide. The environmental sources of As are both geogenic and anthropogenic. Anthropogenic As inputs into the atmosphere and hydrosphere, primarily caused by coal burning and smelting of ores, equal or even surpass geogenic As inputs (Matschullat, 2011). Mining and metallurgical processing of sulfide ores result in contamination point sources characterized by high to extremely high As concentrations in soils and mining wastes (up to tens of g/kg As). At such concentrations, As is sequestered in crystalline As minerals and mineraloids, which are defined as X-ray amorphous, metastable natural materials with a poorly defined structure and variable chemical composition. The desired long-term storage of As in As mineral(oid)s, however, is oftentimes only transient because unfavorable changes in physicochemical conditions in soils or mining wastes induced by, for example, oxidative weathering or soil flooding, trigger the release of As into the aquatic environment. Especially As mineraloids exert a major control on As mobility and bioavailability in soils and aquatic environments. They are common in As-rich ores or mining wastes, and transform into crystalline As phases with time. Yet, the structure of these abundant materials as well as processes by which they (trans)form in natural environments are still poorly understood. This understanding, however, is of economic relevance as it facilitates the evaluation and prediction of the geochemical stability of As-rich mining wastes. In order to remedy the present situation, we proposed a multi-method study of a suite of natural X-ray amorphous ferric arsenates (AFA). In the past, we have investigated the (local) structure of synthetic AFA with a well-defined composition ($FeAsO_4 \times nH_2O$) using EXAFS spectroscopy and total X-ray scattering (Mikutta et al., 2013a,b, 2014). These studies indicated that AFA synthesized at low pH (~2) has a scorodite ($FeAsO_4 \times 2H_2O$)-like local structure, in which each arsenate tetrahedron is corner-linked to four FeO_6 octahedra and vice versa. To date, detailed structure analyses specific to natural AFA are scarce. As opposed to synthetic samples, natural AFA possess highly variable chemical compositions, which provide a record of formation and alteration processes of their geological past. We have collected a set of natural AFA from Jáchymov (Czech Republic), Chyžné (Slovakia), and Rotgülden (Austria), which were analyzed by Fe K-edge X-ray absorption spectroscopy (XAS) at beamline BM20A of ESRF. For spectra comparisons we also synthesized a large set of Fe(III)-As(V) coprecipitates from Fe(III) sulfate and nitrate as a function of pH and Fe/As molar ratio.
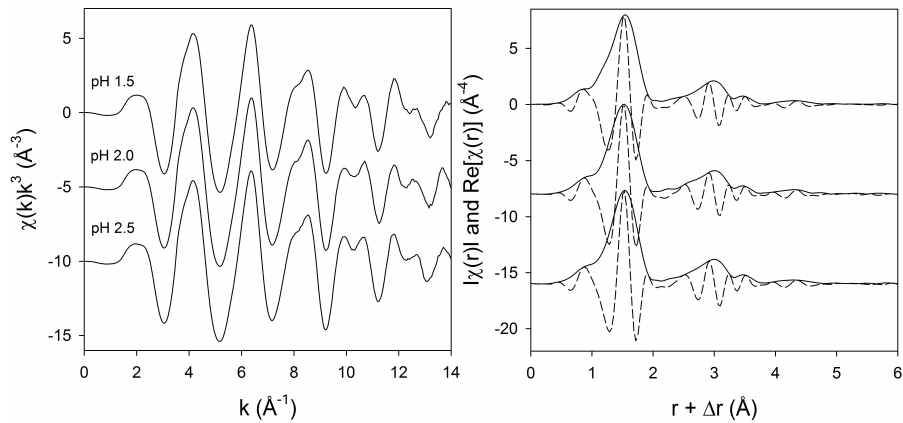
2. Experimental methods and preliminary results

Iron(III)-As(V) coprecipitates were synthesized at pH 1.5-8 and with initial Fe/As molar ratios of 0.8-8.0. Stock solutions containing As(V) ($AsHNa_2O_4 \times 7H_2O$) and Fe(III) ($Fe_2O_{12}S_3 \times 5.6H_2O$ or $Fe(NO_3)_3 \times 9H_2O$) were prepared by keeping the concentration of Fe(III) fixed at 160 mM, and adjusting the concentration of As(V) to attain the target Fe/As molar ratio. The pH of the starting solutions was adjusted to pH 1.1 with conc. H_2SO_4 (sulfate system) or HNO_3 (nitrate system). The solutions were added into a glass beaker by a peristaltic pump at a maximum flow rate of 10 mL/min and kept under constant agitation with a magnetic stirrer ($23\pm1°C$). The pH in the reactor was kept constant at the target value by adding CO_2-free 1 M NaOH using an automated titration system (Titrando 851, Metrohm, Switzerland). After equilibration for one hour at constant pH in their mother liquors, the precipitates formed were repetitively washed with doubly deionized water (18.2 MΩ cm, MilliQ) until the electric conductivity was generally lower than 50 μS/cm, shock-frozen in liquid N_2, and freeze-dried. The dried precipitates were milled with agate mortar and pestle and stored in a desiccator until XAS analysis.
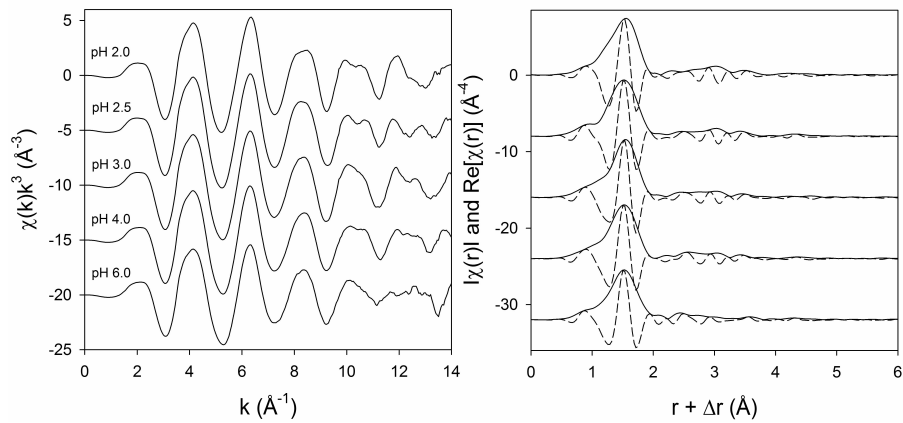
Natural AFA and synthetic Fe(III)-As(V) coprecipitates were analyzed as pressed powder pellets after appropriate dilution with BN to achieve an edge step, μx, of unity. The samples were investigated by Fe K-edge (7112 eV) XANES and EXAFS spectroscopy (up to $k = 16$ Å^{-1}) utilizing the energy resolution of the Si(111) double-crystal monochromator. The monochromator was calibrated by setting the first inflection point of the K-absorption edge of elemental Fe to 7112 eV. The metal foil was simultaneously measured with the samples in order to correct for slight energy shifts during the measurements. Higher harmonics in the beam were reduced by Si mirrors and monochromator detuning (40%). All samples were measured at cryogenic temperature (~15 K) using a He cryostat. The spectra were processed in Athena (Ravel and Newville, 2005) using standard procedures. The Autobk algorithm was applied for background removal using a linear pre-edge line between 200 and 50 eV before the edge, E_0, and a normalization range of 150-970 eV ($E-E_0$). The edge energy, E_0, was defined as zero crossing of the second XANES derivative. By default a quadratic polynomial was used as a post-edge line. The frequency cut-off parameter, R_{bkg}, was set to 0.9, and the k-weight in the background function determination was set to two. Fourier transforms of the spectra were calculated over $k = 2.5$-13.0 Å^{-1} using a Kaiser-Bessel window function with a sill width of 3 Å^{-1}. In total we measured three natural AFA samples, 24 'sulfate-system' and 6 'nitrate-system' Fe(III)-As(V) coprecipitates. Figure 1 displays EXAFS spectra and their Fourier transforms of natural AFA. The spectra generally show similar features but also slight differences in the amplitude ratios beyond approximately $k = 8$ Å^{-1}. Figures 2-4 illustrate EXAFS spectra of synthetic Fe(III)-As(V) coprecipitates synthesized from ferric sulfate salt at varying pH and with initial Fe/As molar ratios of 0.8, 2.4, and 4.8. Among all synthetic Fe(III)-As(V) coprecipitates, those produced from ferric sulfate salt at pH <3 and an initial Fe/As molar ratio of 0.8 showed EXAFS features most similar to the natural AFA samples (cp. Figure 1 and 2). In order to obtain information on the local Fe coordination in all samples, we will analyze the spectra by detailed shell fitting. The shell-fit models will need to be constrained by information on the samples' elemental composition and pair distribution functions (PDF) calculated from high-energy total X-ray scattering data, which will be collected in December 2015 at beamline 11-ID-B of the Advanced Photon Source (APS, Argonne, IL, USA).
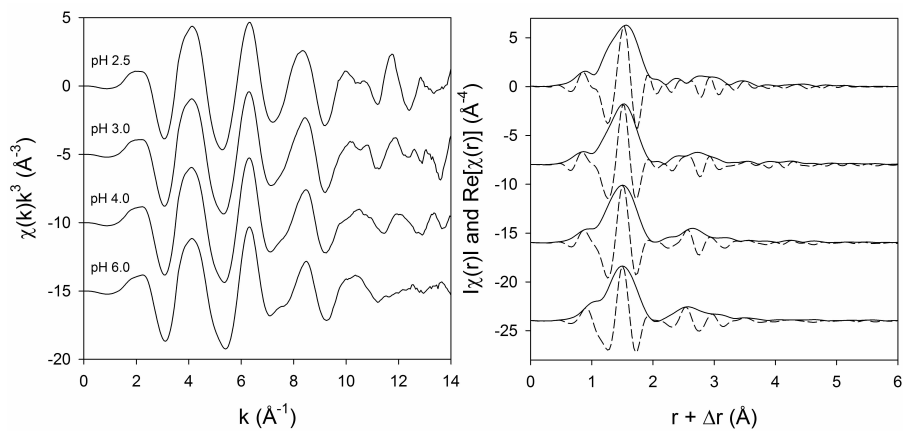

Figure 1. Iron K-edge EXAFS spectra of natural AFA (left) and their corresponding Fourier-transform magnitudes and real parts (right).

Figure 2. Iron K-edge EXAFS spectra of synthetic Fe(III)-As(V) coprecipitates synthesized with an initial molar Fe/As ratio of 0.8 as a function of pH (sulfate system) (left) and their corresponding Fourier-transform magnitudes and real parts (right).

Figure 3. Iron K-edge EXAFS spectra of synthetic Fe(III)-As(V) coprecipitates synthesized with an initial molar Fe/As ratio of 2.4 as a function of pH (sulfate system) (left) and their corresponding Fourier-transform magnitudes and real parts (right).

Figure 4. Iron K-edge EXAFS spectra of synthetic Fe(III)-As(V) coprecipitates synthesized with an initial molar Fe/As ratio of 4.8 as a function of pH (sulfate system) (left) and their corresponding Fourier-transform magnitudes and real parts (right).

3. References

Matschullat J. (2011) In: Deschamps E. and Matschullat J. (eds) *Arsenic: Natural and Anthropogenic*. CRC Press and Balkema. p. 3-26.

Mikutta C., Mandaliev P. N., Kretzschmar R. (2013a) *Environ. Sci. Technol.* **47**, 3122-3131.

Mikutta C., Mandaliev P. N., Kretzschmar, R. (2013b) *Environ. Sci. Technol.* **47**, 13201-13202.

Mikutta C., Schröder C., Michel F. M. (2014) *Geochim. Cosmochim. Acta* **140**, 708-719.

Ravel B., Newville M. (2005) *J. Synchrotron Radiat.* **12**, 537-541.

4. Acknowledgments